Article

Thermal and Mechanical Properties of Recyclable Composites Prepared from Bio-Olefins and Industrial Waste

Perla Y. Sauceda-Oloño [1], Ana C. Borbon-Almada [2], Martin Gaxiola [2], Ashlyn D. Smith [1], Andrew G. Tennyson [1,3,*] and Rhett C. Smith [1,*]

[1] Department of Chemistry and Center for Optical Materials Science and Engineering Technology, Clemson University, Clemson, SC 29634, USA; psauced@g.clemson.edu (P.Y.S.-O.)

[2] Departamento de Ingenieria Civil y Minas, Universidad de Sonora, Hermosillo 83000, Sonora, Mexico; ana.borbon@unison.mx (A.C.B.-A.); martin.gaxiola@unison.mx (M.G.)

[3] Department Materials Science and Engineering, Clemson University, Clemson, SC 29634, USA

* Correspondence: atennys@clemson.edu (A.G.T.); rhett@clemson.edu (R.C.S.)

Abstract: Ordinary Portland Cement (OPC) production consumes tremendous amounts of fresh water and energy and releases vast quantities of CO_2 into the atmosphere. Not only would an alternative to OPC whose production requires no water, releases little CO_2, and consumes less energy represent a transformative advance in the pursuit of industrial decarbonization, but the greater availability of safe drinking water would lead to significantly improved public health, particularly among vulnerable populations most at risk from contaminated water supply. For any OPC alternative to be adopted on any meaningful scale, however, its structural capabilities must meet or exceed those of OPC. An inverse vulcanization of brown grease, sunflower oil, and elemental sulfur (5:5:90 weight ratio) was successfully modified to afford the high-sulfur-content material **SunBG$_{90}$** in quantities > 1 kg, as was necessary for standardized ASTM and ISO testing. Water absorption (ASTM C140) and thermal conductivity (ISO 8302) values for **SunBG$_{90}$** (<1 wt% and 0.126 $W \cdot m^{-1} \cdot K^{-1}$, respectively) were 84% and 94% lower than those for OPC, respectively, suggesting that **SunBG$_{90}$** would be more resistant against freeze-thaw and thermal stress damage than OPC. Consequently, not only does **SunBG$_{90}$** represent a more environmentally friendly material than OPC, but its superior thermomechanical properties suggest that it could be a more environmentally robust material on its own merits, particularly for outdoor structural applications involving significant exposure to water and seasonal or day/night temperature swings.

Keywords: sustainable composite; fats and oils; sulfur; ASTM testing; ISO testing; polymer cement

1. Introduction

Concrete serves critical functions in nearly all aspects of human civilization. The composites that comprise concrete are produced by the mixing of a cementitious binder, most commonly ordinary Portland cement (OPC), aggregates, and water. In the US alone, the annual concrete production exceeds 500 million tons, with the concomitant consumption of nearly 90 million tons of OPC and 250 billion liters of water [1–4]. This demand is driven by the facts that concretes (*i*) can be poured and shaped, unlike natural stone, and (*ii*) have vastly superior mechanical properties compared to those of bricks and other shapeable masonries [2,5–7].

Unfortunately, concrete production has a tremendously harmful impact on the environment. For example, nearly 1 ton of CO_2 is released directly into the atmosphere for each ton of OPC produced and, furthermore, OPC production requires temperatures > 1400 °C, with an electricity demand that indirectly releases even more CO_2 into the atmosphere. Additionally, concrete production can only use fresh water, and this reduces the availability of potable water for human consumption [2]. Concretes cannot be recycled and reused in the same applications as initially poured concretes due to having significantly worse

mechanical strengths. As a result, vast quantities of concretes end up in landfills. Thus, there is an urgent need for concrete alternatives that (*i*) produce less CO_2, or even none at all, (*ii*) do not consume water, and (*iii*) can be recycled and reused without any loss in their mechanical properties.

Given the enormous carbon footprint, energy demand, and water consumption required for the production of OPC, the development of alternatives to OPC is an area of intense interest in the scientific community. In particular, if an OPC alternative could be produced from biomatter without the need for any inorganic carbonates, then it would enable the production of concretes that could formally remove CO_2 from the atmosphere (i.e., so-called "carbon-negative" materials) [8]. A critical constraint in the design of every OPC alternative is that it must match or exceed the mechanical properties of OPC itself and of OPC-derived concretes. Most biomolecules and biopolymers, by nature, must not impair the microscopic or macroscopic flexibility and motility of an organism, and thus, nearly all streams of unmodified biomatter exhibit significantly worse compressive strengths than OPC. If covalent bonds that crosslink individual biomolecules or biopolymer chains could be introduced into biomatter, then this process could yield materials with mechanical strength properties comparable to or superior to OPC.

Inverse vulcanization, mechanistically similar to Goodyear's vulcanization of rubber (Scheme 1a) [9] is a process developed by Pyun in 2013 that crosslinks olefinic molecules with chains of polymeric sulfur and affords high-sulfur-content materials (HSMs, Scheme 1b) that exhibit remarkable thermomechanical properties [10–14]. Notably, the syntheses of HSMs by inverse vulcanization do not require water, or any other solvent, and require lower temperatures than other C–S bond-forming processes reported for the synthesis of HSMs [15–23]. Furthermore, their relatively high sulfur contents (typically > 50 wt%) prevent any water penetration into, or uptake by, HSMs due to the inherent hydrophobicity of sulfur [24–29]. A water-repellent alternative to OPC, furthermore, could preclude entirely some of the degradation/damage pathways that afflict OPC-based concretes [30–35].

Our group [36–38] and others [18,20,39–44] have extensively studied multiple classes of bio-olefins as the organic substrates in inverse vulcanization reactions to produce HSMs with commercially viable thermomechanical properties. Triglycerides and free fatty acids [45,46] are of particular interest to us as components of OPC alternatives given that many of them naturally contain C=C bonds and thus do not require chemical functionalization. If plant-based triglycerides are the only organic substrates in an inverse vulcanization reaction, then the resulting HSM could formally achieve a negative carbon footprint.

A potential issue for the manufacture of HSMs is that when scale-up to kilogram quantities is undertaken, there is the potential for temperature spikes resulting from autoacceleration (the Trommsdorf effect) [47,48]. The previous reports indicate that a possible remedy to temperature control issues is to use rapid mechanical stirring, rather than the magnetic stirring used in small bench top-scale reactions, and to monitor internal reaction temperature rather than external heating bath temperatures as is often done for small-scale reactions.

We have previously reported $SunBG_{90}$ [49], an HSM produced from the inverse vulcanization of a mixture of brown grease and sunflower, and provided data that showed that its compressive strength and flexural strength values were more than 100% greater than the respective values in OPC, and significantly higher than in other analogous plant oil- or terpene-derived HSMs [50,51]. Based on these findings, we sought to scale up the synthesis of $SunBG_{90}$ significantly to enable more rigorous mechanical strength tests based on ASTM- and ISO-certified methods. Herein we report the synthesis of $SunBG_{90}$ to prepare multikilogram-scale prototypes and the shaping of $SunBG_{90}$ into tiles and bricks suitable for ASTM/ISO analyses. Our tests demonstrate that $SunBG_{90}$ is superior to OPC in multiple aspects, with 84% lower water absorption, 94% lower thermal conductivity, and an abrasion resistance between those of marble and granite.

(a)

(b)
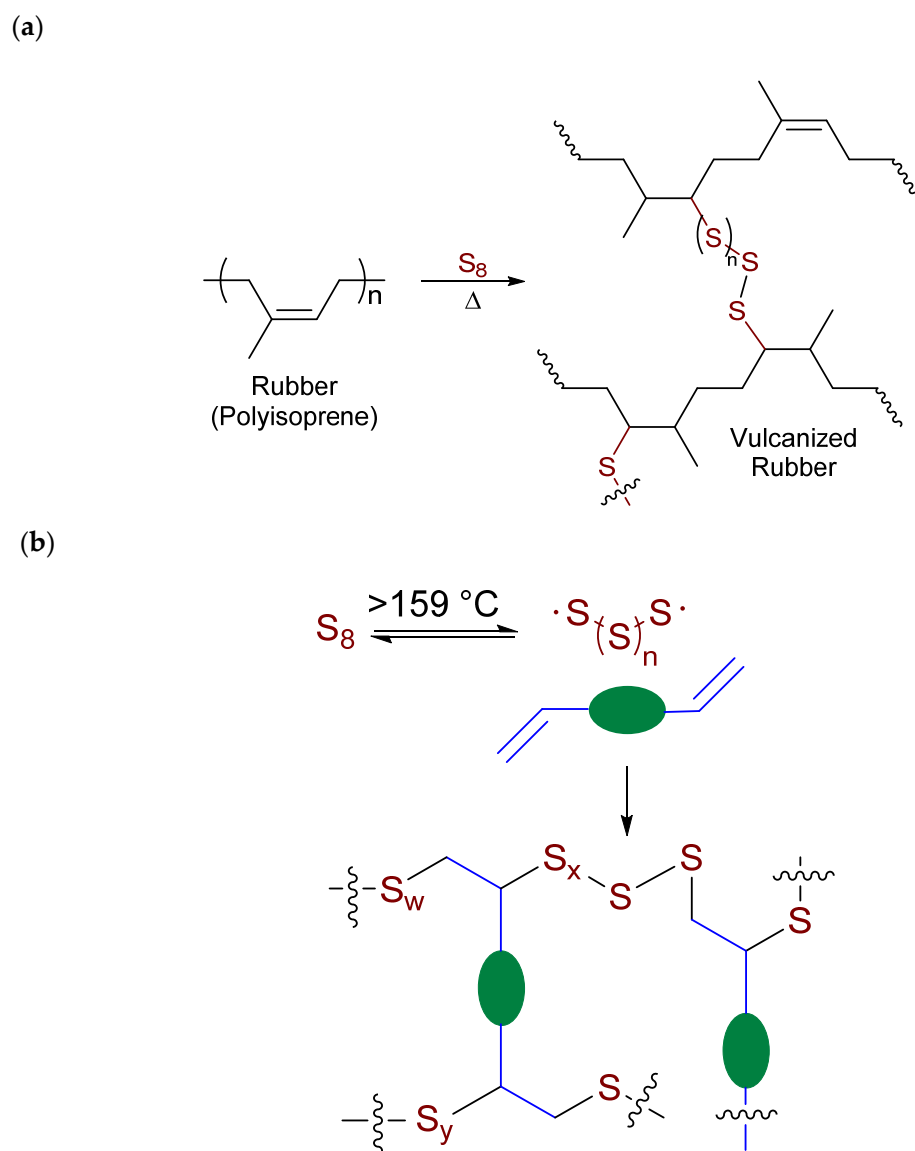
Scheme 1. (**a**) Goodyear vulcanization and (**b**) Pyun inverse vulcanization processes.

2. Materials and Methods

2.1. Materials and Precautions

Small batches (<100 g) of SunBG$_{90}$ can be prepared as previously reported [49]. Caution must be taken during this process, as heating elemental sulfur with organics can result in the formation of H$_2$S gas. H$_2$S is toxic, foul-smelling, and corrosive. The preparation of SunBG$_{90}$ in the large batches that were needed to prepare multi-kilogram prototypes such as the brick used for the ISO 8302 test involved a reaction of sunflower oil, brown grease, and sulfur in a 1:1:18 mass ratio, according to the following procedure, in order to achieve material identical to that resulting from the previously reported small batches. Sulfur was first melted in an oil bath at 160 °C with rapid mechanical stirring. The internal temperature was then increased to 180 °C over 30 min. Once the temperature had stabilized, brown grease was slowly added to the sulfur while stirring and monitoring the temperature. No increase in temperature beyond the typical ±3 °C was observed. After the addition of brown grease was complete, the sunflower oil was added dropwise to the brown grease–sulfur mixture in an analogous manner, again with minimal (±3 °C) temperature variation. The reaction mixture was subsequently stirred for an additional 24 h at 180 °C. After this time a homogeneous reddish-black solution was observed. Upon

cooling to room temperature, the material solidified to a dark solid identified herein as SunBG$_{90}$ in quantitative yield.

2.2. Testing According to ASTM C140

Specimens were immersed in deionized water (temperature range: 15–27 °C) for 24 to 28 h such that the top surfaces of the specimens were at least 150 mm below the surface of the water. Specimens were separated from each other and from the bottom of the tank by at least 3 mm. Samples were weighed before immersion, while suspended by a metal wire and completely submerged in water, and after removal from water. After saturation, the specimens were dried in a ventilated oven at 110 ± 5 °C for not less than 24 h, and the weights of the dried specimens were recorded. The utilized test describes the quantity of water a unit can maintain when saturated, indicating a concrete mix's level of compaction or the volume of voids within a specimen. The primary metric used to measure water absorption is the water absorption rate, typically measured as a percentage of the dry weight of the tile.

$$Absorption, \% = \frac{w_s - w_d}{w_d} \times 100$$

$$Density\ (D), \frac{lb}{ft^3} = \frac{w_d}{w_s - w_i} \times 62.4$$

2.3. Testing According to ASTM C1353

A specimen was abraded using rotary rubbing action under controlled pressure conditions and abrasive action. The test specimen was mounted on a turntable platform and turned on a vertical axis against the sliding rotation of two abrading wheels. One abrading wheel rubbed the specimen outward toward the periphery and the other rubbed it inward toward the center while a vacuum system removed wear debris generated during the test. The resulting abrasion marks formed a crossed arc pattern over an area of approximately 30 cm^2. Abrasion resistance was evaluated by determining the loss of volume due to abrasion and calculating an index of abrasion resistance. This test method allowed the quantification of the abrasion resistance of dimension stone for relation to end-use performance, which is used to comparatively rank material performance.

2.4. Testing According to ISO 8302

The measurement of the thermal conductivity of the material under study was carried out with the Thermal Conductivity Test Tool λ-Meter EP500e according to ISO 8302, which describes the use of guarded hot plate apparatus that offers measurement accuracy < 1.0% in the range λ = 10–60 mW/(m·K) (mostly < 0.7%) and reproducibility < 0.5% (mostly < 0.2%). This meter features a cooling/heating unit with 12 high-performance air-cooled Peltier modules. The material was placed in the center of the sample holder plate of the equipment, which closed automatically, applying a pressure of 500 Pa and thus ensuring complete contact with the temperature plates. A guard of insulating material had to be placed around the sample. The equipment had means of visualization and controls through touch screens.

2.5. Testing According to Mohs Hardness Test

The Mohs hardness scale was used to measure the scratch resistance of a material. The idea behind the Mohs hardness scale is quite simple: the hardest material scratches the softest material. The Mohs hardness scale is based on a scale from 1 to 10, with diamond—which has a value of 10—being the hardest material. Materials are tested against each other; if one scratches another, it has a higher value on the Mohs hardness scale.

3. Results and Discussion

3.1. Rationale and Design

One of the principal challenges associated with the use of bio-olefins in plastics, concretes, or other structural materials is that most bio-olefins are major components

of foodstuffs and contain significant caloric value to both humans as well as animals. Using an edible bio-olefin to prepare an inedible plastic, for example, trades a reduction in CO_2 released for an increase in food insecurity. Brown grease, on the other hand, is a coproduct of animal rendering processes that is not suitable for consumption and is frequently disposed of by incineration, releasing CO_2 into the atmosphere. The inedibility of brown grease is caused in part by the high levels of free fatty acids it contains, which can exceed 30% by weight. By using brown grease as the bio-olefin feedstock in HSM syntheses via inverse vulcanization, there can be a significant decrease in the carbon footprint of animal-derived foodstuff production.

Inverse vulcanization reactions cannot proceed unless the bio-olefin is sufficiently miscible in molten elemental sulfur. To improve the miscibility of brown grease, our protocols dictated that we combine it with a plant-based triglyceride in a 1:1 ratio. Although triglycerides contain significant caloric value, obtaining them from plant-based sources maximizes the amount of CO_2 removed from the atmosphere. Conversely, sulfur is produced by petroleum refining, which is a net CO_2 producer, but millions of tons of elemental sulfur go unused every year and are instead discarded as solid waste [10,44,49,52–57]. Using inverse vulcanization to crosslink the bio-olefins thus has the additional beneficial environmental effect of actively reducing the amount of solid waste that has already accumulated in landfills.

Our group previously demonstrated that $SunBG_{90}$—an HSM prepared via the combination of 5 wt% brown grease, 5 wt% sunflower oil, and 90 wt% sulfur [49]—exhibited a compressive strength value (35.9 MPa, Table 1) that was more than double the compressive strength values of OPC (minimum of 17 MPa required for building foundations), clay bricks (10 MPa), oak wood (11 MPa), marble (12.5 MPa), and limestone (10 MPa). As evidence that brown grease does contribute to mechanical strength, rather than simply diluting the contribution of sunflower oil, it was found that the compressive strengths of $CanBG_{90}$ (identical to $SunBG_{90}$ but with canola oil in place of sunflower oil) [52] and $SunBG_{90}$ were more than double that of the analogous HSM comprising only sunflower oil, $SunS_{90}$ (17.9 MPa). The inclusion of sunflower oil with brown grease was, however, previously reported to be required for the effective mixing of brown grease and sulfur to form a homogeneous material [52].

Table 1. Compressive and flexural strength values for $SunBG_{90}$ and comparison to other materials.

Materials	Compressive Strength (MPa *)	Flexural Strength (MPa *)
$SunBG_{90}$	35.9	7.7
OPC	17	3.7
Clay Bricks	10	3.55
Oak Wood	11	56.5
Marble	12.5	3.4
Limestone	10	2.8
SunS	17.9	ND
$CanBG_{90}$	32.0	6.5

* Numerical values represent maximum values per material.

In the current work, it was also of interest to evaluate the durability of $SunBG_{90}$ after exposure to low temperature and temperature changes. $SunBGS_{90}$ was thus evaluated after 4 d at $-25\ °C$ followed by a rapid return to room temperature. Following this thermal strain, cylinders of $SunBG_{90}$ showed no changes in their compressive strengths compared to the cylinders that were allowed to stand at room temperature prior to testing.

3.2. Synthesis and Fabrication

To prepare bricks and tiles of sufficient sizes for ASTM and ISO testing, the sizes of test samples fabricated from $SunBG_{90}$ had to be scaled up by a factor of over one hundred compared to prior reports. Previous scale-up studies on HSMs had revealed the potential for temperature spikes resulting from autoacceleration (i.e., the Trommsdorf effect) [22,23]

that could be attenuated by using rapid mechanical stirring and fastidious monitoring of internal reaction temperature as reagents were mixed. These precautions were also effective and necessary to produce large batches of $SunBG_{90}$. Indeed, carrying out the large-scale preparation of $SunBG_{90}$ without these temperature control measures had led to the generation of H_2S gas and a material with 70% lower compressive strength than had been observed for previously reported small-scale (<100 g) preparations of $SunBG_{90}$. The careful control of reaction temperature employed in the current report effectively produced $SunBG_{90}$ having identical thermal, mechanical, and morphological properties to those $SunBG_{90}$ samples previously reported.

Tile- and brick-shaped $SunBG_{90}$ substrates for water absorption and density (ASTM C140), abrasion resistance (ASTM C1353) [58,59], thermal conductivity (ISO 8302) [60,61], and Mohs hardness testing [62–64] were prepared by pouring the molten HSM into the appropriate silicone mold and allowing each substrate to solidify gradually at room temperature. Tiles of $SunBG_{90}$ for water absorption and density tests were obtained from molds with dimensions of 2 in × 2 in × 0.25 in (Figure 1). For abrasion resistance tests, the necessary tiles were obtained from larger molds with dimensions of 4 in × 4 in × 0.25 in. For tests of compressive strength, cylinders with dimensions of 10 mm × 6 mm were prepared.

3.3. Water Absorption and Density (ASTM C140)

In routine construction applications, water absorption by various OPC samples, as measured by ASTM C140, typically falls in the range of 5.3–8.3 wt% (Table 2). Water absorption values above this range can cause dangerous decreases in OPC compressive strength that may lead to structural failures [65–67]. Water absorption by **$SunBG_{90}$** was dramatically lower (0.83 wt%) than that by OPC, and intermediate of the absorptivity values for marble and limestone (0.12 and 1.0 wt%, respectively). The density of **$SunBG_{90}$**, measured using ASTM C140, was 1.70 g·cm^{-3}, a value that was significantly lower than that of any of the construction materials listed in Table 2 besides oak. However, the density of **$SunBG_{90}$** did fall within the range of values considered acceptable for lightweight concretes (1.12–1.92 g·cm^{-3}); thus, $SunBG_{90}$ could potentially function as a drop-in replacement for OPC-containing lightweight concretes.
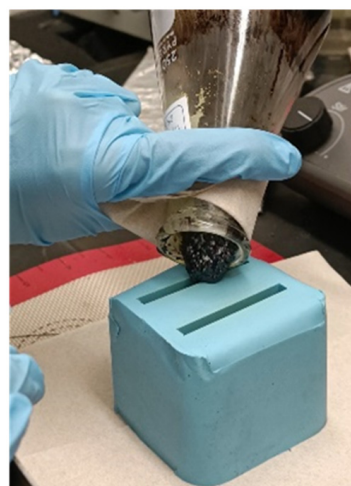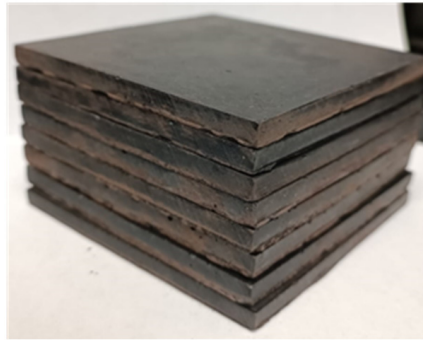
(**a**)

Figure 1. *Cont.*

(b)

(c)

Figure 1. Shaping of SunBG$_{90}$ by pouring a molten sample into silicone mold (**a**) to produce tiles (**b**). A similar process can be used to produce a variety of other shapes such as the cylinders that were used for compressive testing (**c**).

3.4. Thermal Conductivity (ISO 8302)

The test of thermal conductivity was carried out on an HSM composite with a square geometry and dimensions of 148.3 × 148.7 mm and 40.6 mm thickness (Figure 2) that was in a dry state and showed relative parallelism and flatness on its sides. The mass of the sample was 1212 g and its bulk density was 1329 kg/m^3. The relative humidity of the environment surrounding the equipment was 36% and the ambient temperature was 14 °C. Three measurements were made, with temperatures of 10 °C, 25 °C, and 40 °C. The results were obtained after 8 hours of measurement, and the polynomial $y = f(t) = 0.3263(T + 123.40)$ was adjusted to obtain the thermal conductivity value of 126.66 mW/(m·K). The result of the thermal conductivity test of the measured sample yielded 0.126 W/m·K, a value falling within the range of values for familiar construction materials (Table 2 [68–74]) such as wood (0.13 W/m·K) and cellular concrete (0.14 W/m·K). These results, summarized in Table 2, show that SunBG$_{90}$ is a material with thermal insulation capacities, surpassing in this capacity other conventional materials such as OPC concrete (2.25 W/m·K), clay bricks (0.9 W/m·K), adobe bricks (0.85 W/m·K), and limestone (0.85 W/m·K). It has been observed that considering the value of the thermal conductivity of this material, it would work very well to cover surfaces that must be thermally insulated, since it exceeds all conventional construction materials based on cement or masonry, approaching only the value of wood.

Table 2. Water absorption, density, and thermal conductivity data.

Materials	Water Absorption (% *)	Density (g/cm^3)	Thermal Conductivity (W/m·K *)
SunBG$_{90}$	0.83	1.70	0.126
OPC	5.3–8.3	3.15	2.25
Clay Bricks	8.22	2.5	0.9
Oak Wood	12	0.82	0.197
Marble	0.12	2.64	2.95
Limestone	1	2.71	0.85

* Numerical values represent maximum values per material.

Figure 2. Pouring molten SunBG$_{90}$ into a foil-lined brick mold (**a**) to form the brick (**b**) used for ISO 8302, with a mass of 1.212 kg (**c**).

3.5. Abrasion Resistance (ASTM C1353) and Mohs Hardness Test

Surface abrasion is a noted vulnerability in OPC, OPC-derived concretes [75–77], and other tile materials, and can be a major pathway by which loss of mechanical strength and structural integrity occurs [78–80]. An initial evaluation of SunBG$_{90}$ for its potential abrasion resistance was undertaken by conducting a quick evaluation of its hardness on the Mohs scale. Table 3 [81] indicates the known Mohs hardness values, showing that SunBG$_{90}$ has qualitative surface scratch resistance comparable to that of copper, gold, or silver and nearing that of marble or limestone. These preliminary tests suggested that SunBG$_{90}$ may be a candidate for reasonably good abrasion resistance.

Table 3. Mohs hardness values.

Materials	H$_{min}$	H$_{max}$
SunBG$_{90}$	2	2.5
Asphalt	1	2
Sulfur	1.5	2.5
Gold	2.5	3
Silver	2.5	3
Marble	3	4
Limestone	3	4

When ASTM C1353 was performed on SunBG$_{90}$, an abrasion resistance value of 16 (I_W, Table 4) was observed. The abrasion resistance of SunBG$_{90}$ was intermediate to that of limestone and granite (10 and 25, respectively); this was particularly impressive given that limestone and granite are composed almost entirely of inorganic oxides and carbonates, whereas the SunBG$_{90}$ prepared for this work could have contained no more than 0.4 wt% of such inorganic substances.

Table 4. Abrasion resistance.

Materials	Abrasion Resistance (I_w, H_A)
SunBG$_{90}$	16
Granite	25
Marble	10
Limestone	10

Values from ASTM C1353 Abrasion Resistance of Dimension Stone Subjected to Foot Traffic Using a Rotary Platform Abrase documentation.

4. Conclusions

We previously demonstrated that brown grease, sunflower oil, and elemental sulfur, in a 5:5:90 mass ratio, underwent inverse vulcanization to yield SunBG$_{90}$, an HSM which exhibited compressive and flexural strengths that exceeded those of OPC. In the present work, we successfully increased the scale of the inverse vulcanization reaction to prepare multikilogram batches of SunBG$_{90}$, thus enabling the thermomechanical properties of SunBG$_{90}$ to be tested according to the same ASTM and ISO standards used for OPC-based concretes.

Water absorption by SunBG$_{90}$ increased the sample mass by <1% when tested according to ASTM C140; this result indicated a value that was five-fold lower than the values typically measured for OPC (5.3–8.3%). The greater hydrophobicity of SunBG$_{90}$, as an alternative to OPC, would significantly diminish the likelihood of freeze-thaw and corrosion damage, which often lead to dangerous structural weaknesses in OPC-based concretes.

The surface abrasion of OPC-based concretes can likewise introduce weaknesses that ultimately result in mechanical failure. In contrast, the abrasion resistance of 16 measured for SunBG$_{90}$, when tested according to ASTM 1353, was intermediate to the values observed for limestone and granite (10 and 25, respectively). The value of 16 for SunBG$_{90}$ is all the more impressive when considering the fact that SunBG$_{90}$ is essentially metal-free (<0.4 wt% metals), whereas limestone contains has nearly 40 wt% metal content.

Thermal stresses, particularly those resulting from large temperature changes in the day/night cycle, can cause significant damage to materials exposed to the outdoors. For SunBG$_{90}$, a thermal conductivity value of 0.126 W·m^{-1}·K^{-1} was measured using ISO 8302; this value was 94% and 87% lower than the corresponding values for OPC and clay bricks, respectively. As a result, the internal volume of SunBG$_{90}$ that undergoes temperature changes is significantly smaller, and thus, there will be fewer potential sites for mechanical failure.

Collectively, these results provide compelling evidence that SunBG$_{90}$ will be dramatically more resistant to the predominant damage mechanisms which most commonly cause structural failures in OPC-based concretes. Thus, not only does SunBG$_{90}$ constitute a carbon-sequestering alternative to the heavy carbon-footprint material OPC, but it is also likely to have superior long-term environmental robustness over OPC-based concretes and thereby decreases risks associated with the structural failures of concrete.

Author Contributions: Conceptualization, R.C.S.; methodology, R.C.S., A.C.B.-A. and M.G.; formal analysis, P.Y.S.-O., A.C.B.-A. and M.G.; investigation, P.Y.S.-O., A.C.B.-A. and M.G.; resources, A.C.B.-A., M.G., R.C.S. and A.G.T.; data curation, A.C.B.-A., M.G. and P.Y.S.-O.; writing—original draft preparation, P.Y.S.-O. and A.G.T.; writing—review and editing, all authors; supervision, R.C.S., A.D.S., A.C.B.-A., M.G. and A.G.T.; funding acquisition, A.C.B.-A., M.G. and R.C.S. All authors have read and agreed to the published version of the manuscript.

Data Availability Statement: Data not available in the manuscript may be requested from the corresponding author (rhett@clemson.edu).

Conflicts of Interest: The authors declare no conflict of interest.

References

1. Andrew, R.M. Global CO_2 emissions from cement production. *Earth Syst. Sci. Data* **2019**, *11*, 1675–1710. [CrossRef]
2. Scrivener, K.L.; John, V.M.; Gartner, E.M. Eco-efficient cements: Potential economically viable solutions for a low-CO_2 cement-based materials industry. *Cem. Concr. Res.* **2018**, *114*, 2–26. [CrossRef]
3. Khongprom, P.; Suwanmanee, U. Environmental benefits of the integrated alternative technologies of the portland cement production: Case study in Thailand. *Eng. J.* **2017**, *21*, 15–27. [CrossRef]
4. Chen, C.; Habert, G.; Bouzidi, Y.; Jullien, A. Environmental impact of cement production: Detail of the different processes and cement plant variability evaluation. *J. Clean. Prod.* **2010**, *18*, 478–485. [CrossRef]
5. Jeong, J.; Choi, J. Adverse outcome pathways potentially related to hazard identification of microplastics based on toxicity mechanisms. *Chemosphere* **2019**, *231*, 249–255. [CrossRef] [PubMed]
6. Cole, M.; Lindeque, P.; Halsband, C.; Galloway, T.S. Microplastics as contaminants in the marine environment: A review. *Mar. Pollut. Bull.* **2011**, *62*, 2588–2597. [CrossRef]
7. Hidalgo-Ruz, V.; Gutow, L.; Thompson, R.C.; Thiel, M. Microplastics in marine environment review of methods for identification and quantification. *Environ. Sci. Technol.* **2012**, *46*, 3060–3075. [CrossRef]
8. Smith, A.D.; Smith, R.C.; Tennyson, A.G. Polymer cements by copolymerization of waste sulfur, oleic acid, and pozzolan cements. *Sust. Chem. Pharm.* **2020**, *16*, 100249. [CrossRef]
9. Goodyear, C. Improvement in India-Rubber Fabrics. US 3633A, 15 June 1844.
10. Chung, W.J.; Griebel, J.J.; Kim, E.T.; Yoon, H.; Simmonds, A.G.; Ji, H.J.; Dirlam, P.T.; Glass, R.S.; Wie, J.J.; Nguyen, N.A.; et al. The use of elemental sulfur as an alternative feedstock for polymeric materials. *Nat. Chem.* **2013**, *5*, 518–524. [CrossRef]
11. Lee, T.; Dirlam, P.T.; Njardarson, J.T.; Glass, R.S.; Pyun, J. Polymerizations with Elemental Sulfur: From Petroleum Refining to Polymeric Materials. *J. Am. Chem. Soc.* **2022**, *144*, 5–22. [CrossRef] [PubMed]
12. Kang, K.-S.; Phan, A.; Olikagu, C.; Lee, T.; Loy, D.A.; Kwon, M.; Paik, H.-j.; Hong, S.J.; Bang, J.; Parker, W.O., Jr.; et al. Segmented Polyurethanes and Thermoplastic Elastomers from Elemental Sulfur with Enhanced Thermomechanical Properties and Flame Retardancy. *Angew. Chem. Int. Ed.* **2021**, *60*, 22900–22907. [CrossRef] [PubMed]
13. Kleine, T.S.; Lee, T.; Carothers, K.J.; Hamilton, M.O.; Anderson, L.E.; Ruiz Diaz, L.; Lyons, N.P.; Coasey, K.R.; Parker, W.O., Jr.; Borghi, L.; et al. Infrared Fingerprint Engineering: A Molecular-Design Approach to Long-Wave Infrared Transparency with Polymeric Materials. *Angew. Chem. Int. Ed.* **2019**, *58*, 17656–17660. [CrossRef]
14. Simmonds, A.G.; Griebel, J.J.; Park, J.; Kim, K.R.; Chung, W.J.; Oleshko, V.P.; Kim, J.; Kim, E.T.; Glass, R.S.; Soles, C.L.; et al. Inverse Vulcanization of Elemental Sulfur to Prepare Polymeric Electrode Materials for Li-S Batteries. *ACS Macro Lett.* **2014**, *3*, 229–232. [CrossRef] [PubMed]
15. Karunarathna, M.S.; Lauer, M.K.; Tennyson, A.G.; Smith, R.C. Copolymerization of an aryl halide and elemental sulfur as a route to high sulfur content materials. *Polym. Chem.* **2020**, *11*, 1621–1628. [CrossRef]
16. Wu, X.; Smith, J.A.; Petcher, S.; Zhang, B.; Parker, D.J.; Griffin, J.M.; Hasell, T. Catalytic inverse vulcanization. *Nat. Commun.* **2019**, *10*, 10035–10044. [CrossRef]
17. Westerman Clayton, R.; Walker Princess, M.; Jenkins Courtney, L. Synthesis of Terpolymers at Mild Temperatures Using Dynamic Sulfur Bonds in Poly(S-Divinylbenzene). *J. Vis. Exp. JoVE* **2019**, *147*, e59620.
18. Yan, P.; Zhao, W.; McBride, F.; Cai, D.; Dale, J.; Hanna, V.; Hasell, T. Mechanochemical synthesis of inverse vulcanized polymers. *Nat. Commun.* **2022**, *13*, 4824. [CrossRef] [PubMed]
19. Westerman, C.R.; Jenkins, C.L. Dynamic Sulfur Bonds Initiate Polymerization of Vinyl and Allyl Ethers at Mild Temperatures. *Macromolecules* **2018**, *51*, 7233–7238. [CrossRef]
20. Tonkin, S.J.; Gibson, C.T.; Campbell, J.A.; Lewis, D.A.; Karton, A.; Hasell, T.; Chalker, J.M. Chemically induced repair, adhesion, and recycling of polymers made by inverse vulcanization. *Chem. Sci.* **2020**, *11*, 5537–5546. [CrossRef]
21. Lundquist, N.A.; Tikoalu, A.D.; Worthington, M.J.H.; Shapter, R.; Tonkin, S.J.; Stojcevski, F.; Mann, M.; Gibson, C.T.; Gascooke, J.R.; Karton, A.; et al. Reactive Compression Molding Post-Inverse Vulcanization: A Method to Assemble, Recycle, and Repurpose Sulfur Polymers and Composites. *Chem.—Eur. J.* **2020**, *26*, 10035–10044. [CrossRef] [PubMed]
22. Smith, J.A.; Green, S.J.; Petcher, S.; Parker, D.J.; Zhang, B.; Worthington, M.J.H.; Wu, X.; Kelly, C.A.; Baker, T.; Gibson, C.T.; et al. Crosslinker Copolymerization for Property Control in Inverse Vulcanization. *Chem.—Eur. J.* **2019**, *25*, 10433–10440. [CrossRef] [PubMed]
23. Dodd, L.J.; Omar, O.; Wu, X.; Hasell, T. Investigating the Role and Scope of Catalysts in Inverse Vulcanization. *ACS Catal.* **2021**, *11*, 4441–4455. [CrossRef]
24. Gutarowska, B.; Piotrowska, M.; Kozirog, A.; Berlowska, J.; Dziugan, P.; Kotynia, R.; Bielinski, D.; Anyszka, R.; Wreczycki, J. New Sulfur Organic Polymer-Concrete Composites Containing Waste Materials: Mechanical Characteristics and Resistance to Biocorrosion. *Materials* **2019**, *12*, 2602. [CrossRef] [PubMed]
25. Meyer, B. Elemental sulfur. *Inorg. Sulphur Chem.* **1968**, *76*, 241–258. [CrossRef]
26. Meyer, B. Solid allotropes of sulfur. *Chem. Rev.* **1964**, *64*, 429–451. [CrossRef]
27. Dehestani, M.; Teimortashlu, E.; Molaei, M.; Ghomian, M.; Firoozi, S.; Aghili, S. Experimental data on compressive strength and durability of sulfur concrete modified by styrene and bitumen. *Data Brief* **2017**, *13*, 137–144. [CrossRef] [PubMed]
28. Weil, E.D. Recent industrial organosulfur chemistry. *Phosphorus Sulfur Silicon Relat. Elem.* **1991**, *59*, 325–340. [CrossRef]
29. Duecker, W.W. Admixtures improve properties of sulfur cements. *Chem. Metall. Eng.* **1934**, *41*, 583–586.

30. Liu, P.; Feng, C.; Wang, F.; Gao, Y.; Yang, J.; Zhang, W.; Yang, L. Hydrophobic and water-resisting behavior of Portland cement incorporated by oleic acid modified fly ash. *Mater. Struct.* **2018**, *51*, 38. [CrossRef]

31. Ksiazek, M.M.K. Evaluation of acid corrosion resistance of Portland cement composites impregnated with polymer sulfur composite. *Anti-Corros. Methods Mater.* **2017**, *64*, 1–15. [CrossRef]

32. Gay, H.; Meynet, T.; Colombani, J. Local study of the corrosion kinetics of hardened Portland cement under acid attack. *Cem. Concr. Res.* **2016**, *90*, 36–42. [CrossRef]

33. Izzat, A.M.; Al Bakri, A.M.M.; Kamarudin, H.; Sandu, A.V.; Ruzaidi, G.C.M.; Faheem, M.T.M.; Moga, L.M. Sulfuric acid attack on ordinary Portland cement and geopolymer material. *Rev. Chim.* **2013**, *64*, 1011–1014.

34. Scrivener, K.L.; Fullmann, T.; Gallucci, E.; Walenta, G.; Bermejo, E. Quantitative study of Portland cement hydration by X-ray diffraction/Rietveld analysis and independent methods. *Cem. Concr. Res.* **2004**, *34*, 1541–1547. [CrossRef]

35. Fattuhi, N.I.; Hughes, B.P. Ordinary portland cement mixes with selected admixtures subjected to sulfuric acid attack. *ACI Mater. J.* **1988**, *85*, 512–518. [CrossRef]

36. Lauer, M.K.; Tennyson, A.G.; Smith, R.C. Green Synthesis of Thermoplastic Composites from a Terpenoid-Cellulose Ester. *ACS Appl. Polym. Mater.* **2020**, *2*, 3761–3765. [CrossRef]

37. Lauer, M.K.; Tennyson, A.G.; Smith, R.C. Inverse vulcanization of octenyl succinate-modified corn starch as a route to biopolymer-sulfur composites. *Mater. Adv.* **2021**, *2*, 2391–2397. [CrossRef]

38. Lauer, M.K.; Karunarathna, M.S.; Tennyson, A.G.; Smith, R.C. Robust, remeltable and remarkably simple to prepare biomass-sulfur composites. *Mater. Adv.* **2020**, *1*, 2271–2278. [CrossRef]

39. Yan, P.; Zhao, W.; Tonkin, S.J.; Chalker, J.M.; Schiller, T.L.; Hasell, T. Stretchable and Durable Inverse Vulcanized Polymers with Chemical and Thermal Recycling. *Chem. Mater.* **2022**, *34*, 1167–1178. [CrossRef]

40. Gupta, A.; Worthington, M.J.H.; Patel, H.D.; Johnston, M.R.; Puri, M.; Chalker, J.M. Reaction of sulfur and sustainable algae oil for polymer synthesis and enrichment of saturated triglycerides. *ACS Sust. Chem. Eng.* **2022**, *10*, 9022–9028. [CrossRef]

41. Eder, M.L.; Call, C.B.; Jenkins, C.L. Utilizing Reclaimed Petroleum Waste to Synthesize Water-Soluble Polysulfides for Selective Heavy Metal Binding and Detection. *ACS Appl. Polym. Mater.* **2022**, *4*, 1110–1116. [CrossRef]

42. Orme, K.; Fistrovich, A.H.; Jenkins, C.L. Tailoring Polysulfide Properties through Variations of Inverse Vulcanization. *Macromolecules* **2020**, *53*, 9353–9361. [CrossRef]

43. Jia, J.; Liu, J.; Wang, Z.-Q.; Liu, T.; Yan, P.; Gong, X.-Q.; Zhao, C.; Chen, L.; Miao, C.; Zhao, W.; et al. Photoinduced inverse vulcanization. *Nat. Chem.* **2022**, *14*, 1249–1257. [CrossRef]

44. Yan, P.; Zhao, W.; Zhang, B.; Jiang, L.; Petcher, S.; Smith, J.A.; Parker, D.J.; Cooper, A.I.; Lei, J.; Hasell, T. Inverse vulcanized polymers with shape memory, enhanced mechanical properties, and vitrimer behavior. *Angew. Chem. Int. Ed.* **2020**, *59*, 13371–13378. [CrossRef]

45. Smith, A.D.; Smith, R.C.; Tennyson, A.G. Sulfur-Containing Polymers Prepared from Fatty Acid-Derived Monomers: Application of Atom-Economical Thiol-ene/Thiol-yne Click Reactions and Inverse Vulcanization Strategies. *Sus. Chem.* **2020**, *1*, 209–237. [CrossRef]

46. Smith, A.D.; McMillin, C.D.; Smith, R.C.; Tennyson, A.G. Copolymers by Inverse Vulcanization of Sulfur with Pure or Technical Grade Unsaturated Fatty Acids. *J. Poly. Sci.* **2020**, *58*, 438–445. [CrossRef]

47. Gerrens, H. Radical reactions in polymerization processes. *Ber. Bunsen-Ges.* **1963**, *67*, 741–753. [CrossRef]

48. Griebel, J.J.; Li, G.; Glass, R.S.; Char, K.; Pyun, J. Kilogram scale inverse vulcanization of elemental sulfur to prepare high capacity polymer electrodes for Li-S batteries. *J. Poly. Sci. Part A Polym. Chem.* **2015**, *53*, 173–177. [CrossRef]

49. Lopez, C.V.; Smith, A.D.; Smith, R.C. High strength composites from low-value animal coproducts and industrial waste sulfur. *RSC Adv.* **2022**, *12*, 1535–1542. [CrossRef]

50. Maladeniya, C.P.; Karunarathna, M.S.; Lauer, M.K.; Lopez, C.V.; Thiounn, T.; Smith, R.C. A Role for Terpenoid Cyclization in the Atom Economical Polymerization of Terpenoids with Sulfur to Yield Durable Composites. *Mater. Adv.* **2020**, *1*, 1665–1674. [CrossRef]

51. Maladeniya, C.P.; Smith, R.C. Influence of Component Ratio on Thermal and Mechanical Properties of Terpenoid-Sulfur Composites. *J. Compos. Sci.* **2021**, *5*, 257. [CrossRef]

52. Lopez, C.V.; Karunarathna, M.S.; Lauer, M.K.; Maladeniya, C.P.; Thiounn, T.; Ackley, E.D.; Smith, R.C. High Strength, Acid-Resistant Composites from Canola, Sunflower, or Linseed Oils: Influence of Triglyceride Unsaturation on Material Properties. *J. Poly. Sci.* **2020**, *58*, 2259–2266. [CrossRef]

53. Zhang, Y.; Glass, R.S.; Char, K.; Pyun, J. Recent advances in the polymerization of elemental sulphur, inverse vulcanization and methods to obtain functional Chalcogenide Hybrid Inorganic/Organic Polymers (CHIPs). *Polym. Chem.* **2019**, *10*, 4078–4105. [CrossRef]

54. Kleine, T.S.; Glass, R.S.; Lichtenberger, D.L.; MacKay, M.E.; Char, K.; Norwood, R.A.; Pyun, J. 100th Anniversary of Macromolecular Science Viewpoint: High Refractive Index Polymers from Elemental Sulfur for Infrared Thermal Imaging and Optics. *ACS Macro Lett.* **2020**, *9*, 245–259. [CrossRef] [PubMed]

55. Worthington, M.J.H.; Kucera, R.L.; Chalker, J.M. Green chemistry and polymers made from sulfur. *Green Chem.* **2017**, *19*, 2748–2761. [CrossRef]

56. Chalker, J.M.; Worthington, M.J.H.; Lundquist, N.A.; Esdaile, L.J. Synthesis and Applications of Polymers Made by Inverse Vulcanization. *Top. Curr. Chem.* **2019**, *377*, 1–27. [CrossRef]

57. Maladeniya, C.P.; Tennyson, A.G.; Smith, R.C. Single-stage chemical recycling of plastic waste to yield durable composites via a tandem transesterification-thiocracking process. *J. Polym. Sci.* **2023**, *61*, 787–793. [CrossRef]

58. Pena-Rodriguez, G.; Dulce-Moreno, H.; Daza-Ramirez, J.; Orozco-Hernandez, S.; Vargas-Galvis, F. Mechanical and tribological behavior of red clay ceramic tiles coated with fly ash powders by thermal spraying technique. *J. Phys. Conf. Ser.* **2017**, *792*, 012026/012021–012026/012026. [CrossRef]

59. Khatwa, M.A.; Salem, H.G.; Haggar, S.M. Building material from waste. *Can. Metall. Q.* **2005**, *44*, 339–350. [CrossRef]

60. Namboonruang, W.; Rawangkul, R.; Yodsudjai, W. A perspective study on strength properties-low thermal conductivity and leachability of Pozzolanics soil bricks towards to environmentally friendly. *Adv. Sci. Lett.* **2013**, *19*, 2831–2841. [CrossRef]

61. Namboonruang, W.; Rawangkul, R.; Yodsudjai, W. Strength properties of low thermal conductivity fly ash bricks: Compressive and flexural strength aspects. *Appl. Mech. Mater.* **2012**, *117–119*, 1352–1357. [CrossRef]

62. Gerberich, W.W.; Ballarini, R.; Hintsala, E.D.; Mishra, M.; Molinari, J.-F.; Szlufarska, I. Toward Demystifying the Mohs Hardness Scale. *J. Am. Ceram. Soc.* **2015**, *98*, 2681–2688. [CrossRef]

63. Goncalves, R.A.; Biasoli de Mello, J.D.; Aguiar, K.M.; Guimaraes da Rosa, F. Evaluation of the wear resistance of ceramic floor tiles by the resistance equivalent to that of Mohs hardness standard materials. *Ceram. Ind.* **2004**, *9*, 23–27.

64. Troeger, E. Remarks on the criticism of the Mohs' scale of hardness. *Neues Jahrb. Fuer Mineral. Mon.* **1954**, *92*, 233–243.

65. Fehervari, A.; Gates, W.P.; Gallage, C.; Collins, F. A Porous Stone Technique to Measure the Initial Water Uptake by Supplementary Cementitious Materials. *Minerals* **2021**, *11*, 1185. [CrossRef]

66. Sugiman, S.; Salman, S.; Maryudi, M. Effects of volume fraction on water uptake and tensile properties of epoxy filled with inorganic fillers having different reactivity to water. *Mater. Today Commun.* **2020**, *24*, 101360. [CrossRef]

67. Rucker-Gramm, P.; Beddoe, R.E. Effect of moisture content of concrete on water uptake. *Cem. Concr. Res.* **2010**, *40*, 102–108. [CrossRef]

68. Čáchová, M.; Koňáková, D.; Vejmelková, E.; Keppert, M.; Černý, R. Mechanical and thermal properties of the Czech marbles. In Proceedings of the AIP Conference Proceedings, Rhodes, Greece, 22–28 September 2015; p. 280010.

69. Çavuş, V.; Şahin, S.; Esteves, B.; Ayata, U. Determination of thermal conductivity properties in some wood species obtained from Turkey. *BioResources* **2019**, *14*, 6709–6715. [CrossRef]

70. Cho, W.J.; Kwon, S.; Choi, J.W. The thermal conductivity for granite with various water contents. *Eng. Geol.* **2009**, *107*, 167–171. [CrossRef]

71. El Fgaier, F.; Lafhaj, Z.; Brachelet, F.; Antczak, E.; Chapiseau, C. Thermal performance of unfired clay bricks used in construction in the north of France: Case study. *Case Stud. Constr. Mater.* **2015**, *3*, 102–111. [CrossRef]

72. Lertwattanaruk, P.; Choksiriwanna, J. The physical and thermal properties of adobe brick containing bagasse for earth construction. *Int. J. Build. Urban Inter. Landsc. Technol. (BUILT)* **2011**, *1*, 57–66. [CrossRef]

73. Rambaldi, E.; Prete, F.; Timellini, G. Thermal and Acoutics Performances of Porcelain Stoneware Tiles. *Qualicer* **2014**, *14*, 1–4.

74. Yun, T.S.; Jeong, Y.J.; Youm, K.-S. Effect of surrogate aggregates on the thermal conductivity of concrete at ambient and elevated temperatures. *Sci. World J.* **2014**, *2014*, 939632. [CrossRef]

75. Wang, Q.; Liu, R.; Liu, P.; Liu, C.; Sun, L.; Zhang, H. Effects of silica fume on the abrasion resistance of low-heat Portland cement concrete. *Constr. Build. Mater.* **2022**, *329*, 127165. [CrossRef]

76. Cheyad, S.M.; Hilo, A.N.; Al-Gasham, T.S. Comparing the abrasion resistance of conventional concrete and geopolymer samples. *Mater. Today: Proc.* **2022**, *56*, 1832–1839. [CrossRef]

77. Negahban, E.; Bagheri, A.; Sanjayan, J. Investigation of abrasion resistance of geopolymer concrete cured in ambient temperature for pavement applications. In *Road Materials and Pavement Design*; Taylor & Francis: London, UK, 2022. [CrossRef]

78. Baigorri Garcia, P. Chemical and abrasion resistance of ceramic glazes for floors. *Ceram. Inf.* **1986**, *21*, 145–149.

79. Skuthan, R. Abrasion resistant glazes for floor tiles. *Interceram* **1977**, *26*, 52–53.

80. Thiel, G.A. Relative resistance to abrasion of mineral grains of sand size. *J. Sediment. Petrol.* **1940**, *10*, 103–124.

81. Tabor, D. Mohs's hardness scale-a physical interpretation. *Proc. Phys. Society. Sect. B* **1954**, *67*, 249. [CrossRef]